*Romanian Reports in Physics, Vol. 66, No. 4, P. 1137–1146, 2014*

# CHARACTERIZATION OF ZIRCONIA THIN FILMS GROWN BY RADIO-FREQUENCY PLASMA ASSISTED LASER ABLATION*

V. N. CANCEA [1], M. FILIPESCU [2,*], G. VELISA[3], V. ION[2], A. ANDREI[2], D. PANTELICA[3], R. BIRJEGA[2], P. IONESCU[3], N. SCINTEE[3], M. DINESCU[2]

[1] University of Craiova, Department of Physics, 200585 Craiova, Romania
[2] National Institute for Lasers, Plasma and Radiation Physics, P.O. Box MG 16, RO 77125 Magurele - Bucharest, Romania
[3] "Horia Hulubei" National Institute of Physics and Nuclear Engineering, P.O.BOX MG-6, Bucharest - Magurele, Romania
*E-mail: mihaela.filipescu@inflpr.ro

*Received September 23, 2013*

*Abstract*. In this work we report on the deposition of zirconia as thin films by Radio-Frequency discharge assisted Pulsed Laser Deposition. The influence of the deposition parameters like substrate temperature and RF presence on the structure and morphology of the deposited layers was studied. Techniques as Atomic Force Microscopy, X-ray Diffraction, Non-Rutherford Backscattering Spectrometry and optical measurements have been used to characterize the deposited layers. It was found that polycrystalline zirconia thin films with uniform surface morphology, holes and cracks free, were obtained at 873 K substrate temperature, for a RF power of 150 W.

*Key words*: crystalline ceramics, zirconia thin films, radio-frequency assisted plasma.

## 1. INTRODUCTION

Nowadays, the nuclear waste management represents a difficult challenge for the industrialized countries. One viable option to eliminate of the excess plutonium arising from nuclear power plants and dismantled nuclear weapons is its incineration in a light-water reactor [1–4]. To that purpose, the concept of an inert matrix fuel has been advanced. Due to their physical and chemical properties, some crystalline ceramics (*i.e.* MgO, CaO, $Y_2O_3$, $ZrO_2$, $CeO_2$) are considered to be potential candidates as diluents for burning of plutonium fuels in nuclear reactors [5]. One of these materials presenting attractive properties is zirconium oxide (or

* Paper presented at the 16th International Conference on Plasma Physics and Applications, June 20–25, 2013, Magurele, Bucharest, Romania.

zirconia). It has a high melting point [6], good mechanical properties, stability under irradiation [7], oxidation resistance, high chemical stability [8], low solubility in water, retention of radiotoxic elements, and adequate neutronic properties [9].

In order to use a small amount of material, but keeping intact the physical and chemical properties, the $ZrO_2$ are obtained as crystalline thin films in the micron/nanometer scale.

Zirconia thin films are at present grown by different techniques: Metal-Organic Chemical Vapour Deposition – MOCVD [10–14], dual frequency sputtering [15], Radio-Frequency Sputtering [16], ultraviolet ozone oxidation [17–19], Atomic Layer Chemical Vapour Deposition – ALCVD [20], Photo-Chemical Vapour Deposition – Photo-CVD [21], sol-gel [22], etc. Some of these methods are quite expensive since they use a large amount of material and are non-stoichiometrically controlled. As an alternative, a laser based method that resolves these issues is Pulsed Laser Deposition – PLD (or laser ablation) [23]. The PLD technique involves the interaction of a laser beam with a target material producing a plume which transports the particles onto a substrate, where a thin film is formed [24]. A problem often met in deposition of oxides thin films is the appearance of oxygen vacancies in the layer and at the layer-substrate interface. This problem can be avoided if to the conventional PLD system is added a Radio-Frequency (RF) discharge at the substrate level. This hybrid technique (RF-PLD) combines the advantages of PLD (clean reactor, low temperature, and high efficiency process) with ‘‘in situ’’ enhancement of the reactivity on the substrate.

The aim of this work is to prove the possibility to grow crystalline thin films of zirconia ceramic using PLD.

The influence of the deposition parameters like substrate temperature and RF presence on the structure and morphology of the deposited layers was studied. Techniques as Atomic Force Microscopy, X-ray Diffraction, Non-Rutherford Backscattering Spectrometry and ellipsometry have been used to characterize the deposited layers.

## 2. EXPERIMENTAL

### 2.1. DEPOSITION SYSTEM

The PLD experimental setup consists in a Nd:YAG laser with four harmonics, a reaction chamber, a pump-system assuring a base pressure of $10^{-4}$ Pa, a target rotation-translation system and a heater (up to 1073 K).

A laser beam with a wavelength of 266 nm hits a zirconia (stabilized with 2.5% of hafnium) ceramic target in order to obtain $ZrO_2$ layers. The pressure of oxygen was maintained at 5 Pa during deposition of all samples.

Single crystal Si(100) plates (1 $cm^2$ samples) were used as collectors. The distance between the target and collector was set at 4 cm. The samples were deposited at different temperatures starting from room temperature (294 K) up to 473 K, 673 K and 873 K. Laser fluence was fixed at 2.5 $Jcm^{-2}$ [25]. The number of laser pulses was varied from 20000 to 60000. A sketch of the experimental setup is shown in [26].

For a considerable improvement of the thin film surface a radio-frequency discharge from a generator working at 13.56 MHz and a maximum power of 1000 W was added to the PLD setup. This discharge leads to an increase in the reactivity on the substrate, due to the ionised and excited species coming from the RF plasma beam. It also acts on the thin layer in the space between the laser pulses when the atoms are settled down to form a thin film [27].

## 2.2. INVESTIGATION METHODS

X-ray Diffraction, Atomic Force Microscopy, Non-Rutherford Backscattering Spectrometry and ellipsometry techniques have been performed in order to characterize the deposited layers.

X-ray diffraction (XRD) was performed using a Panalytical X'Pert PRO system in Bragg-Brentano geometry. The diffractions peaks were identified according to JCPDS files no 41-1164 for the tetragonal $ZrO_2$ and no 34-1484 for the monoclinic $ZrO_2$. The grain sizes were evaluated using the Debye-Scherrer formula.

In order to investigate the surface of zirconia thin films, an Atomic Force Microscope (AFM) scanning in intermittent mode was used.

Ellipsometric investigations were performed with a Woollam Variable Angle Spectroscopic Ellipsometer (VASE) system, equipped with a high pressure Xe discharge lamp incorporated in an HS-190 monochromator. Optical measurements were performed in the visible and near-UV region of the spectrum at wavelengths between 400 and 1700 nm, step of 5 nm at 60° and 80° incidence angles. Bulk refractive indices for the silicon substrates and for the native silicon oxide were taken from literature [30]. A native $SiO_2$ of 3 nm results from the fitting procedure in the case of Si substrates. The optical model consisted in 4 layers in the case of the films deposited on Si: the substrate, the native $SiO_2$ (3 nm), the $ZrO_2$ layer and a rough top layer which was set to have half air and half $ZrO_2$.

The Non-Rutherford Backscattering Spectrometry (NRBS) measurements were carried out at the Van de Graaff tandem accelerator (8.5 MV). A beam of $^4He^+$ at 4.5 MeV was used. The backscattered ions were detected using a Si detector, placed at 167° with respect to the beam. The energy resolution of the RBS setup (~17 keV) corresponds to an in-depth resolution of ~12 nm. The spectra were analysed by the RUMP [28] simulation computer program. The upper energies at which the backscattering cross section can still be predicted by the Rutherford scattering formula are 2.5 and 3.7 MeV for oxygen and silicon, respectively.

The cross sections for alpha particles backscattering on O and Si were extracted from the Ion Beam Analysis Nuclear Data Library (IBANDL) [29] and were implemented in the RUMP simulation code.

## 3. RESULTS AND DISCUSSIONS

The XRD pattern of the ceramic target exhibits a predominant tetragonal phase (lattice parameters $a$ = 0.361 nm $c$ = 0.518 nm, tetragonality $c/a$ = 1.43) and traces of a monoclinic phase. Upon after deposition of all samples the XRD performed on the ablated target surface reveals increased intensities of the tetragonal phase, due to re-crystallization processes. The monoclinic phase almost disappeared. The lattice parameters remain the same as before the ablation. The XRD patterns of $ZrO_2$ thin films deposited by PLD under the same conditions except the substrate temperature disclose the strong dependence of the crystallinity of the thin films with the substrate temperature (Fig. 1).

The XRD patterns show the formation of a dominant tetragonal zirconia phase beginning with the film deposited on the substrate heated at 673 K. The peaks appeared better resolved and sharper for the thin film deposited on the 873 K heated substrate. The XRD peaks are assigned to the (101) and to the (002) peaks of the tetragonal phase. The absence of other peaks shows a preferred orientation growth.

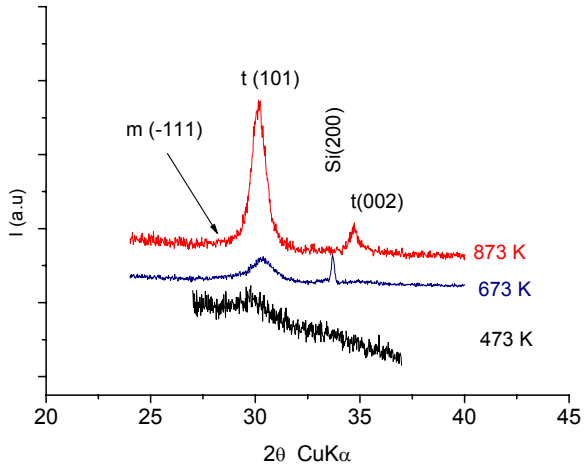


Fig. 1 – The XRD patterns of the $ZrO_2$ thin films on Si (100) substrate heated at different temperatures. 20000 pulses were used for the deposition of the thin films.

By increasing the number of pulses sent to the target, thin films with an increased thickness are obtained. The effect is observed in the corresponding XRD spectra by an almost linear increase of the peak intensities with the number of

pulses (Fig. 2). This indicates the formation of crystalline thin films with a thickness direct proportional with the number of pulses sent to the target. However, there is some anisotropy of the growth in the crystallographic directions as the ratio of the $I_{002}/I_{101}$ intensities denotes (Fig. 3).

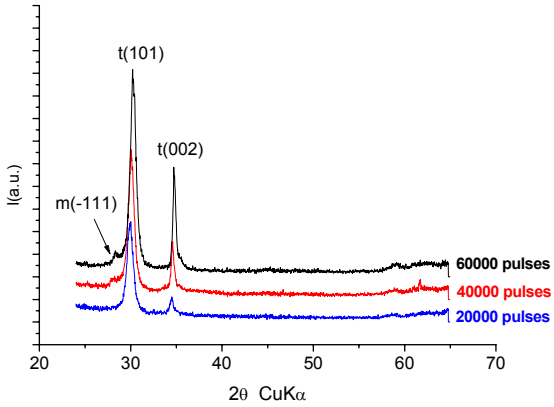


Fig. 2 – XRD patterns of $ZrO_2$ thin films deposited on 873 K heated substrate. The films are obtained at different number of pulses sent on the target.

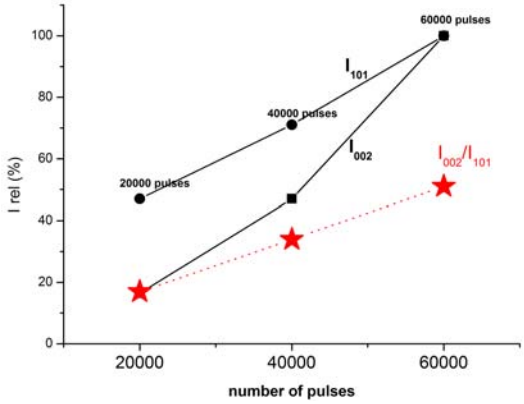


Fig. 3 – The evolution of the (101) and (002) peak intensities normalized to the intensities of films deposited at 60000 pulses, indicative of the formation of crystalline thin films with a thickness proportional to the number of pulses sent to the target. The $I_{002}/I_{101}$ ratio for the same films deposited using different number of pulses is also included, marking an anisotropy of the growth along different crystallographic directions.

Traces of a monoclinic phase, namely the (–111) peak, are more clearly observed in thicker films.

For target and zirconia thin films, the evaluation of the grain size in the two crystallographic directions also reveals differences in the dimensions of the crystalline domain along these two directions (Table 1). The results could be

associated with the presence of defects which are anisotropically distributed. We mention that small crystallite sizes, especially in the main crystallographic growth direction (101), could be related to the thermal stabilization of the tetragonal phase.

*Table 1*

Grain sizes for zirconia target and samples obtained by PLD at different substrate temperature

| No. sample | Substrate temp. [K] | No pulses | $D_t$ (101) [nm] | $D_t$ (002) [nm] |
|---|---|---|---|---|
| target | | | 34 | 34 |
| 1 | 673 | 20000 | 7 | 10 |
| 2 | 873 | 20000 | 11 | 23 |
| 3 | 873 | 40000 | 11 | 24 |
| 4 | 873 | 60000 | 11 | 18 |

AFM investigations revealed smooth and uniform surfaces, without cracks and pores, with only few droplets, on all PLD deposited samples.

The influence of the substrate temperature on the morphological properties of zirconia nanostructure thin films is presented in Fig. 4. Increasing the temperature from 294 K to 873 K, the surface morphology did not show an important change: only few droplets were observed and the roughness value was around 6 nm for all thin films.

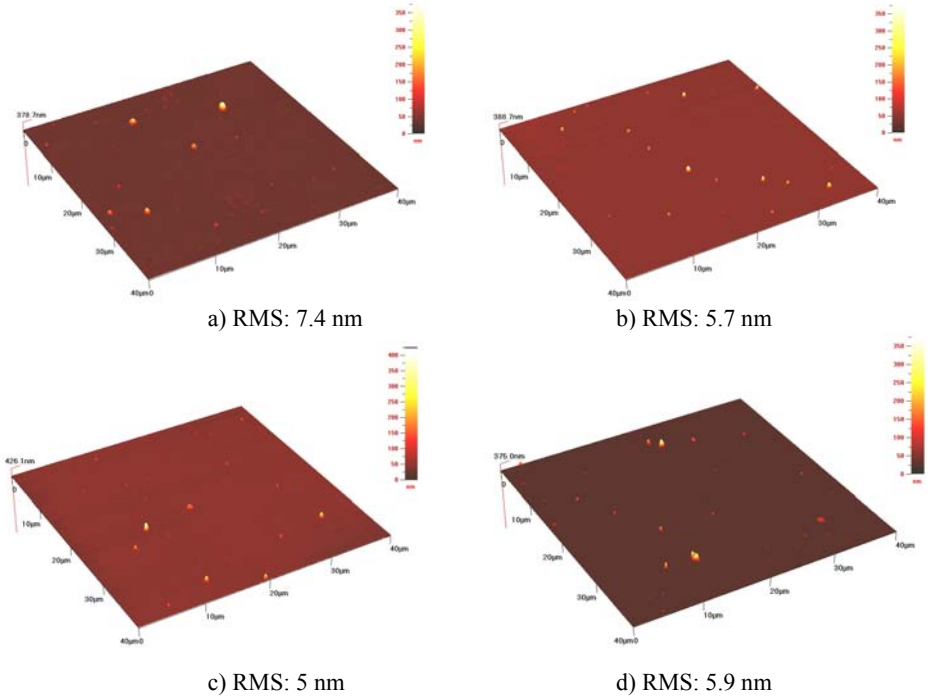

a) RMS: 7.4 nm b) RMS: 5.7 nm

c) RMS: 5 nm d) RMS: 5.9 nm

Fig. 4 – The AFM images of zirconia thin films grown by simple PLD on Silicon substrate at 5 Pa oxygen, laser fluence of 2.5 J/cm$^2$, 20.000 laser pulses at: a) 294 K; b) 473 K; c) 673 K; d) 873 K.

The radio-frequency discharge added to the PLD system leads to an improvement of zirconia thin films surfaces. Zirconia layers grown by RF-PLD present smaller values of the surface roughness with smaller droplets than those grown by PLD under the same conditions (473 K substrate temperature, 5 Pa oxygen, and laser fluence of 2.5 Jcm$^{-2}$). Also, the droplets density decreases in the case of zirconia thin films obtained by RF-PLD (Fig. 5).

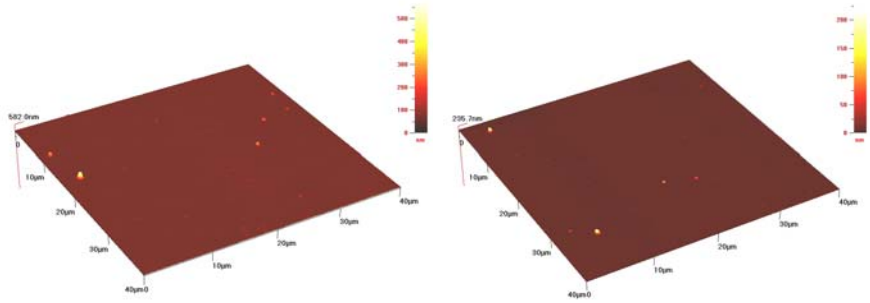

a) RMS: 6.9 nm b) RMS: 3.1 nm

Fig. 5 – The AFM images of zirconia thin films grown at 473 K, 5 Pa oxygen, laser fluence of 2.5 Jcm$^{-2}$ by: a) simple PLD; b) RF-PLD.

The film and rough layer thicknesses and refractive indices were obtained by fitting the data in the 400 nm − 1700 nm range at various temperatures using a Cauchy function [31, 32], $n(\lambda) = A_n + B_n / \lambda^2$. The $n$ is refractive index, $\lambda$ is wavelength in nanometres, and $A_n$ and $B_n$ are constant coefficients. In this range the $ZrO_2$ thin film is non-absorbing ($k = 0$) [33] and such dispersion is accepted. For a sample growth at 873 *K*, target being irradiated with 40,000 laser pulses, without RF plasma discharge, $A_n$ = 2.1486 ± 0.000549, $B_n$ = 0.023251 ± 0.000163, thickness is 104.129 ± 0.0712 nm and roughness is 1.874 ± 0.125 nm.

The spectroscopic ellipsometry analyses show different refractive indices for the samples grown at different substrate temperatures (Fig. 6). The $n$ values of the films growth at 873 K are higher that the $n$ values for the film obtained at room temperature. This behaviour is observed for the two sets of samples (grown in the presence or without RF plasma). A possible explanation is that the thin films grown at higher temperature (> 473 K) present crystalline phases, while those grown at room temperature are amorphous.

NRBS (Non-Rutherford Backscattering Spectrometry) technique was used to determine the stoichiometry and thickness of $ZrO_2$ layers on silicon.

In Fig. 7 is presented a NRBS spectrum of the $ZrO_2$/Si thin film, measured with a $^4$He beam ($E$ = 4.5 MeV). An enhanced O peak is present due to the oxygen contained in the zirconia film. Some small peaks are observed in the Si signal

region due to resonances of the non-Rutherford $^{28}Si(\alpha,\alpha)^{28}Si$ cross-section; these are taken into account in the simulation. The result of a simulation using the RUMP code is presented with continuous line. The simulated and experimental backscattering spectra show quite good agreement. The composition of zirconia layer deduced from alpha backscattering spectrum is: $ZrO_2Hf_{0.012}$.

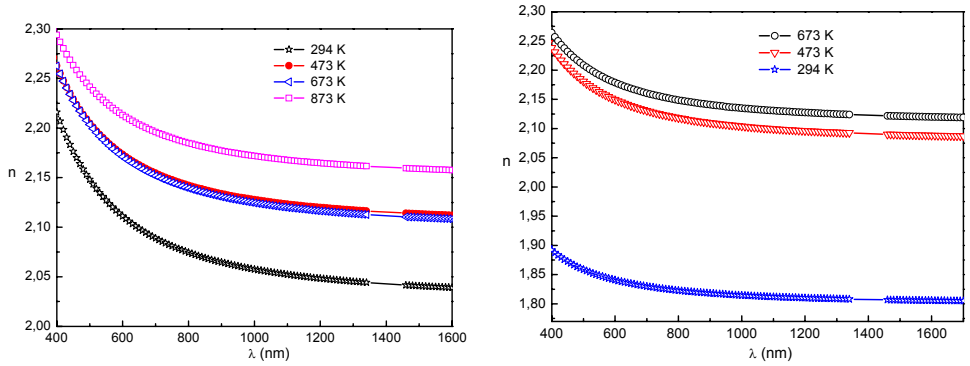


a) b)

Fig. 6 – Refractive indices for the $ZrO_2$ thin film growth at different temperatures by: a) PLD; b) RF-PLD.

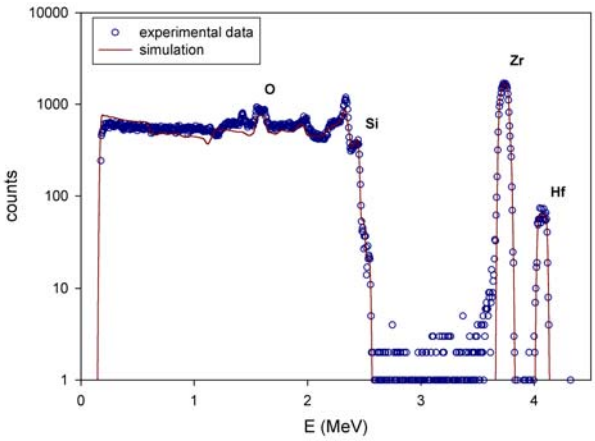


Fig. 7 – RBS spectra for a thin film deposited on silicon substrate at 600°C, 5 Pa oxygen and laser fluence of 2.5 J/cm$^2$.

## 4. CONCLUSIONS

The XRD patterns show the formation of a dominant tetragonal zirconia phase starting with the film deposited at 673 K substrate temperature. The peaks

appeared better resolved and sharper for the thin film deposited at 873 K. The XRD peaks are assigned to the (101) and (002) peaks of the tetragonal phase.

By increasing the temperature from 294 K to 873 K, the surface morphology did not show significant differences: rare droplets were observed and the roughness value is around 6 nm for all the layers. The composition of zirconia layer deduced from alpha backscattering spectrum was of $ZrO_2Hf_{0.012}$.

The radio-frequency discharge added to the PLD system leads to an improvement of the zirconia thin films surfaces: smaller roughness and smaller size of droplets than in the case of thin films grown by PLD only.

***Acknowledgments***. One of the authors (V.N.C.) acknowledges support from the strategic grant POSDRU/159/1.5/S/133255, Project ID 133255 (2014), co-financed by the European Social Fund within the Sectorial Operational Program Human Resources Development 2007–2013.

## REFERENCES

1. V. M. Oversby, C. C. McPheeters, C. Degueldre, J. M. Paratte, J.Nucl. Mater., **245**, 17–26 (1997).
2. C. Degueldre, J. M. Paratte, Nucl. Technol., **123**, 21–29 (1998).
3. K. E. Sickafus, Hj. Matzke, Th. Hartmann, K. Yasuda, J. A. Valdez, P. Chodak III, M. Nastasi, R. A. Verrall, J. Nucl. Mater., **274**, 66–77 (1999).
4. W. L. Gong, W. Lutze, R. C. Ewing, J. Nucl. Mater., **277**, 239–249 (2000).
5. H. Kleykamp, J. Nucl. Mater., **275**, 1–11 (1999).
6. R. Stevens, *Zirconia and zirconia ceramics*, Magnesium Elektron Ltd, Twickenham, 1986.
7. L. Thomé, A. Gentils, J. Jagielski, F. Garrido, T. Thomé, Nucl. Instr. Meth., **B 250**, 106–113 (2006).
8. L. Thomé, A. Gentils, J. Jagielski, F. Garrido, T. Thomé, Vacuum, **81**, 1264–1270 (2007).
9. C. Degueldre, J. Alloy Compd. **444–445**, 36–41 (2007).
10. J. Shappir, A. Anis, I. Pinsky, IEEE Trans. Electron Devices, **ED-33**, 442–449 (1986).
11. G. Garcia, J. Casado, J. Llibre, A. Figueras, J. Cryst. Growth, **156**, 426–432 (1995).
12. K. Galicka-Fau, C. Legros, M. Andrieux, M. Brunet, J. Szade, G. Garry, Appl. Surf. Sci., **255**, 8986–8994 (2009).
13. A. M. Torres-Huerta, M. A. Domínguez-Crespo, E. Ramírez-Meneses, J. R. Vargas-García, Appl. Surf. Sci., **255**, 4792–4795 (2009).
14. M. Brunet, H. Mafhoz Kotb, L. Bouscayrol , E. Scheid, M. Andrieux, C. Legros, S. Schamm-Chardon, Thin Solid Films, **519**, 5638–5644 (2011).
15. Y. Ohtsu, Y. Hino, H. Fujita, M. Akiyama, K. Yukimura, Vacuum, **83**, 1364–1367 (2009).
16. H. Tomaszewski, J. Haemers, J. Denul, N. De Roo, R. De Gryse, Thin Solid Films, **287**, 104–109 (1996).
17. S. Ramanathan, G. D. Wilk, D. A. Muller, C. M. Park, P. C. McIntyre, Appl. Phys. Lett., **79**, 2621–2623 (2001).
18. S. Ramanathan, P. C. McIntyre, Appl. Phys. Lett., **80**, 3793–3795 (2002).
19. S. Ramanathan, D. A. Muller, G. D. Wilk, C. M. Park, P. C. McIntyre, Appl. Phys. Lett., **79**, 3311–3313 (2001).
20. M. Copel, M. Gribelyuk, E. Gusev, Appl. Phys. Lett., **76**, 436–438 (2000).
21. J. J. Yu, I. W. Boyd, Appl. Phys., **A 75**, 489–491 (2002).
22. N. Petkova, S. Dlugocz, S. Gutzov, J. Non-Cryst. Solids, **357**, 1547–1551 (2011).
23. D. B. Chrisey, G. K. Hubler, *Pulsed laser deposition of thin films*, John Wiley & Sons, New York, 1994, 115.

24. D. Brodoceanu, N. D. Scarisoreanu, M. Filipescu, G. N. Epurescu, D. G. Matei, P. Verardi, F. Craciun, M. Dinescu, *Plasma production by laser ablation 2003*, World Scientific, Singapore, 2004, 41–46.
25. I. Vrejoiu, D. G. Matei, M. Morar, G. Epurescu, A. Ferrari, M. Balucani, G. Lamedica, G. Dinescu, C. Grogoriu, M. Dinescu, Mat. Sci. Semicon. Proc., **5**, 253–257 (2003).
26. M. Filipescu, N. Scarisoreanu, V. Craciun, B. Mitu, A. Purice, A. Moldovan, V. Ion, O. Toma, M. Dinescu, Appl. Surf. Sci., **253**, 8184–8191 (2007).
27. G. Dinescu, D. Matei, D. Brodoceanu, N. Scarisoreanu, M. Morar, P. Verardi, F. Craciun, O. Toma, J. D. Pedarnig, M. Dinescu, Proc., SPIE **5448**, 136–143 (2004).
28. L. R. Doolittle, Nucl. Instr. Meth., B **9**, 344–351 (1985).
29. *** www-nds.iaea.org/ibandl
30. C. M. Herzinger, B. Johs, W. A. McGahan, J. A. Woollam, W. Paulson, J. Appl. Phys., **83**, 3323–3336 (1998).
31. L. Cauchy, Bull. Sci. Math., **14**, 6–10 (1830).
32. H. G. Tompkins, W. A. McGaham, *Spectroscopic ellipsometry and reflectometry*, John Wiley & Sons, New York, 1999.
33. D. Ciuparu, A. Ensuque, G. Shafeev, F. Bozon-Verduraz, J. Mater. Sci. Lett., **19**, 931–933 (2000).